ACS Macro Letters

Letter

pubs.acs.org/macroletters

Nanofiber Polyplex Formation Based on the Morphology Elongation by the Intrapolyplex PEG Crowding Effect

Ryuta Aono, Eiji Yuba, Atsushi Harada,* and Kenji Kono

Department of Applied Chemistry, Graduate School of Engineering, Osaka Prefecture University, 1-1 Gakuen-cho, Naka-ku, Sakai, Osaka 599-8531, Japan

Supporting Information

ABSTRACT: We prepared a multiarm poly(ethylene glycol)-poly(L-lysine) block copolymer (maPEG-PLL) with a size-controllable maPEG head and a cationic PLL tail for the evaluation of the effect of maPEG crowding to the polyplex formation with plasmid DNA. maPEG-PLLs of various compositions were synthesized and the formation of a polyplex was confirmed by gel retardation assay. The maPEG-PLL exhibited non-cooperative polyplex formation behavior, suggesting the effective hydration of the polyplex. Also, an increase in the size of the maPEG head induces the elongation of polyplex morphology from spherical aggregates to nanorods and nanofibers because of the intrapolyplex PEG crowding effect. Furthermore, an increase in the size of the maPEG head also improves the effective inhibition of the decrease in cell-free gene expression, indicating the importance of the control of pDNA packaging in the polyplex.

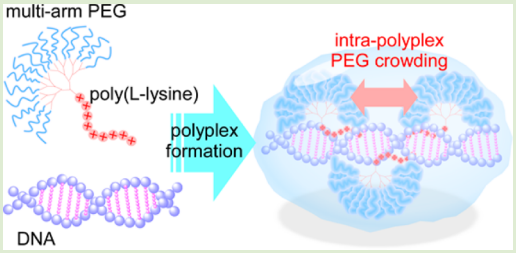

Self-assemblies of block copolymers in selective solvents have recently received considerable attention from both fundamental and applied points of view.[1] In the case of block copolymers composed of hydrophilic and hydrophobic blocks, block copolymer self-assemblies are formed by a hydrophobic interaction in the aqueous medium. Block copolymer self-assemblies can have various morphologies, including spherical, rod, and lamellar structures, and can be controlled by the chemical structure and the composition of the block copolymer and the solvent quality. The spherical self-assembly of block copolymers, that is, polymeric micelles, has potential utility in a drug delivery system (DDS). Many studies have focused on the application of polymeric micelles as carriers of hydrophobic drugs.[2] In these studies, the properties of shell-forming blocks, that is, hydrophilic blocks in block copolymers, are crucial to determine the performance of the polymeric micelles as drug carriers. Poly(ethylene glycol) (PEG) is often used as a shell-forming block because of its good biocompatibility based on the effective exclusion volume effect. Polymeric micelles from block copolymers bearing PEG blocks as the shell-forming blocks can have a long blood circulation time and can effectively accumulate in tumors by the control of the size of the polymeric micelles. Such an effect of PEG was also observed for polyplexes formed between plasmid DNA and cationic block copolymers bearing a PEG block.[3] Kataoka et al. investigated polyplex formation from plasmid DNA with various kinds of cationic block copolymers bearing a PEG block.[4] They recently reported that PEG crowdedness significantly correlated to blood retention profile, showing the critical role of shape and the systemic circulation property for the polyplexes of plasmid DNA and PEG-*block*-poly(L-lysine).[3] However, they only evaluated the effect of poly(L-lysine) length, which directly interact with DNA, on the fixed molecular weight of the PEG block (M_n = 12000), and there exists no report on the effect of the size of the PEG block. Also, Kissel et al. reported the polyplex formation of siRNA with branched poly(ethylene imine)-*graft*-linear PEG (PEI-*g*-PEG) bearing various molecular weight of PEG.[5] They confirmed that PEI-*g*-PEG could form spherical polyplexes with siRNA and long PEG grafts decreased in the aggregation of the polyplexes in AFM observation.

We studied a head−tail type polycation composed of a polyamidoamine (PAMAM) head and a poly(L-lysine) (PLL) tail, in which the end of the PLL tail was attached to the focal point of a PAMAM dendron head, as a nonviral gene vector.[6] The effective stabilization of PAMAM dendron-PLL polyplexes against incubation with serum proteins by the introduction of PEG chains to the periphery of a PAMAM dendron head has recently been successfully undertaken. As a result of the effective stabilization of polyplexes, a PEG-installed PAMAM dendron-PLL, which has a multiarm PEG head and a PLL tail (maPEG-PLL), has been shown to have comparable transfection efficiency to polyethyleneimine polyplexes. In these studies, we found that maPEG-PLL effectively inhibits the condensation of plasmid DNA regardless of the complexation, in which DNA condensation was determined by dye exclusion assay using EtBr.[6d] maPEG-PLL has the inhibition ability of DNA condensation and this unique ability of maPEG-PLL might come from the crowding effect of the maPEG head. Regardless of only indirect interaction with DNA of maPEG head, the size of maPEG might influence not only DNA

Received: February 3, 2014
Accepted: March 20, 2014
Published: March 24, 2014

   dx.doi.org/10.1021/mz500072k | *ACS Macro Lett.* 2014, 3, 333−336

condensation but also other properties of the polyplexes, including morphology and transfection efficiency, regardless of interacting with DNA indirectly. We thus evaluated the size effect of the maPEG head in maPEG-PLL on polyplex formation and the morphology of the polyplexes. We also confirmed that nanofiber polyplex formation was due to the crowding effect of maPEG heads within a polyplex.

maPEGs with different exclusion volumes were synthesized using a PAMAM dendron of the third and fourth generation and PEGs with a number-average molecular weight (M_n) of 2000 and 5000. The successful synthesis of maPEGs with different exclusion volumes was confirmed by GPC measurements (Supporting Information, Figure S1). The radius of gyration (R_g) of the obtained maPEG was calculated from the M_n determined using the calibration curve for linear PEG, as summarized in Table 1, since the R_g of maPEG corresponds to the R_g of linear PEG bearing same exclusion volume. Using maPEGs with varying R_g, the ring-opening polymerization of ε-benzyloxycarbonyl-L-lysine [Lys(Z)] N-carboxy anhydride was initiated from the amino group at the focal point of the maPEGs. After the polymerization, the benzyloxycarbonyl groups in the side chain were removed by acid treatment using 30% HBr/HCl. The synthesis of maPEG-PLLs was confirmed by ^{1}H NMR and GPC measurements, and the maPEG-PLLs prepared here are abbreviated as *XY-Z* from PEG M_n (*X* = 2k and 5k), the number of PEG arms (*Y* = 8 and 16), and the polymerization degree of PLL (*Z*; Table 1).

Table 1. Characteristics of the maPEG-PLLs

	maPEG head			
code (*XY-Z*)	M_n of PEG arm	number of arms	R_g[a] (nm)	PD of PLL tail
2k8−72	2000	8	1.59	72
2k16−36	2000	16	2.02	36
2k16−75	2000	16	2.02	75
2k16−140	2000	16	2.02	140
5k8−66	5000	8	2.45	66
5k16−71	5000	16	3.13	71

[a] R_g was calculated from $\alpha(N/6)^{1/2}$ with α being the segment length (α = 0.29 for PEG) and N is the polymerization degree, which was determined from the GPC data using a calibration curve of linear PEGs.[7]

The polyplex solutions were prepared by mixing pDNA and maPEG-PLL solutions, after pDNA and the maPEG-PLL were separately dissolved in phosphate buffered saline (PBS). The polyplexes were stored for at least overnight before the evaluation. The polyplex formation of pDNA with various types of polycations was evaluated by gel retardation assay. Figure 1 shows electrophoretic images of mixtures of pDNA with maPEG-PLL and PLL, in which the *N*/*P* ratio was defined as the number of Lys residues against the number of phosphate groups of pDNA. Two types of polyplex formation mechanism, that is, cooperative and noncooperative, were observed. In the former, the band intensity for naked pDNA gradually decreased with an increase in the *N*/*P* ratio without a change in the migration distance (Figure 1a), indicating all or none type polyplex formation. On the other hand, in the latter the migration distance in the electrophoretic image gradually shortened with an increase in the *N*/*P* ratio, as typically shown in Figure 1b, indicating a gradual neutralization of the pDNA molecules. The mixture of pDNA with maPEG-PLL, excluding 2k16−140, exhibits noncooperative behavior, and the mixture of pDNA with 2k16−140 and PLL exhibits cooperative behavior. The condensation of pDNA is principally caused by charge neutralization upon polyion complexation with cationic compounds. Negatively charged pDNA is hydrated in solution with a spatially expanded conformation due to the positive osmotic pressure originating from electrostatic repulsion, entropic elasticity, solvation of the DNA chain, counterions, and mixing entropy. Upon complexation, counterions are released into solution leading to an increase in translational entropy, and this is the main driving force for complexation. At the same time, the dehydrated DNA chain accommodates negative osmotic pressure resulting in condensation into a compact form, which decreases the surface free energy. The difference in polyplex formation behavior might be induced by differences in the DNA condensation process since there is no significant difference in the release of counterions at the same mixing charge ratio. The conformation of the pDNA molecule is restricted upon complexation, and this phenomenon is a thermodynamic disadvantage. The degree of this disadvantage determines the cooperativity of polyplex formation. That is, when the entropic disadvantage is relatively small, the polycation chains maintain a random distribution relative to the pDNA molecules. In this case, the electrophoretic image showed a stepwise change in migration distance with an increase in the *N*/*P* ratio, indicating the gradual neutralization of the pDNA molecules, that is, noncooperative polyplex formation, as shown in Figure 1b. Several reports exist concerning noncooperative polyplex formation. Using polycations similar to maPEG-PLL, Maruyama et al. reported on noncooperative polyplex formation using poly(L-lysine) bearing dextran grafts.[8] A common feature is that the polycation has a hydrophilic part with a relatively high weight fraction. The hydrophilic part provides effective hydration in the polyplexes, and this can play an important role in noncooperative polyplex formation.

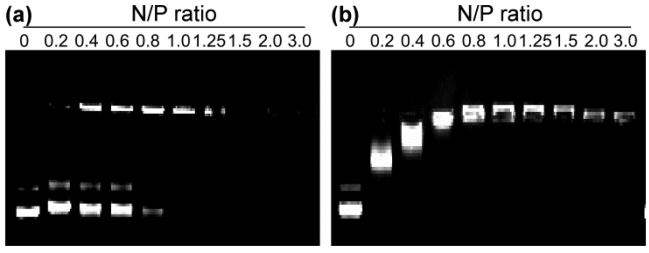

Figure 1. Agarose gel electrophoretic images for the evaluation of polyplex formation: (a) PLL and (b) 5k8−66.

The gel retardation assay shown in Figure 1 suggests that maPEG-PLL can undergo noncooperative polyplex formation because of the relatively low entropic loss with the retardation of pDNA conformation by neutralization. pDNA molecules are large molecules compared with polycation chains, and the conformation of pDNA can strongly influence the morphology of the polyplexes. To evaluate the effect of maPEG size on polyplex morphology, the morphology of the polyplexes prepared using maPEG-PLL with various compositions was observed by atomic force microscopy (Figure 2). Three types of morphologies, including spherical aggregates, nanorods, and nanofibers, were observed. To determine the effect of polymer composition on polyplex morphology, the major and minor axis lengths (L_{maj} and L_{min}) of the polyplexes were measured and

dx.doi.org/10.1021/mz500072k | ACS Macro Lett. 2014, 3, 333−336

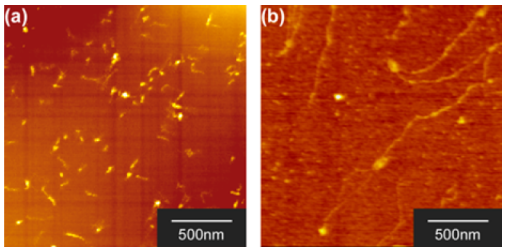

Figure 2. Atomic force microscopy images of nanorod and nanofiber polyplexes prepared using 5k8−66 (a) and 5k16−71 (b). The polyplexes were prepared at N/P = 3.

the aspect ratio (L_{maj}/L_{min}) was calculated as indications of morphology (Table 2). Figure 3a shows the aspect ratio (L_{maj}/L_{min}) distribution for the polyplexes prepared using maPEG-PLL bearing the same maPEG and different PLL lengths. For the 2k16−36 and 2k16−75 polyplexes, the aspect ratio of the polyplexes are widely distributed from 1 to 10, indicating the formation of spherical aggregates and nanorods. On the other hand, 2k16−140 bearing the longest PLL mainly formed spherical aggregates and more than 80% of the polyplexes with the aspect ratio equal to or less than 2. The PLL length in maPEG-PLL influenced the polyplex morphology, as shown in Figure 3. This trend was similar to that reported by Kataoka et al. using linear PEG-PLL. A decrease in PLL length causes the crowding of PEGs, and this might affect polyplex morphology.

Table 2. Major and Minor Axis Lengths of Polyplexes Prepared Using maPEG-PLLs at N/P = 3

	axis length[a] (nm ± SD)		
code (*XY-Z*)	major (L_{maj})	minor (L_{min})	aspect ratio (L_{maj}/L_{min})
2k8−72	194 ± 54	139 ± 23	1.40
2k16−36	317 ± 240	99 ± 33	3.19
2k16−75	428 ± 261	142 ± 43	3.02
2k16−140	203 ± 82	133 ± 30	1.53
5k8−66	355 ± 54	106 ± 22	3.35
5k16−71	965 ± 247	88 ± 15	11.03

[a]The axis length of 100 poyplexes for each type of polyplex are measured in AFM images.

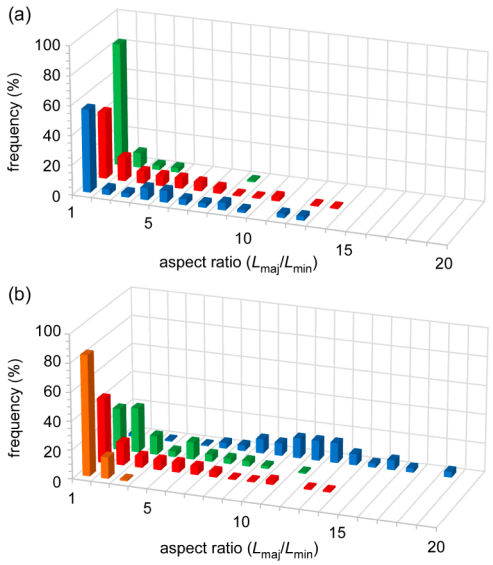

Figure 3. Aspect ratio distribution of the polyplexes prepared from maPEG-PLL with various compositions. (a) Effect of PLL tail length. Blue, red, and green bars present 2k16−36, 2k16−75, and 2k16−140, respectively. (b) Effect of maPEG head size. Orange, red, green, and blue bars represent 2k8−72, 2k16−75, 5k8−66, and 5k16−71, respectively. The aspect ratio of 100 polyplexes are determined for each type of polyplex. The polyplexes were prepared at N/P = 3.

The size effect of the maPEG head on polyplex morphology was also evaluated using maPEG-PLL with different sizes of maPEGs and a similar PLL length. Figure 3b shows the aspect ratio distribution for the polyplexes prepared using 2k8−72, 2k16−75, 5k8−66, and 5k16−71 in which these maPEG-PLLs have different sizes of maPEGs (1.59 nm < R_g < 3.13 nm), as summarized in Table 1. Obviously the distribution of the aspect ratio shifted with an increase of R_g of maPEG head. Eventually, the maPEG-PLL with the largest maPEG head (5k16−71) almost exclusively formed nanofiber polyplexes, and the average aspect ratio reached 11.03. A decrease in the PLL length and an increase in the size of the maPEG head in maPEG-PLL can result in the crowding of the maPEG head in the polyplexes. When the DNA molecule is neutralized by polycations, the DNA molecule can shrink due to a decrease of the electrostatic repulsion. The elongation of polyplex morphology observed here might be due to the effective inhibition of DNA molecule shrinkage through effective hydration by maPEG heads. For nanorod polyplex formation using linear PEG-PLL, it has been reported that nanorod structures are formed with a quantized length of $1/2(n + 1)$ that of the original pDNA length by folding n times, and the pDNA folding process is determined by the rigidity of the double-stranded DNA structure and the topological restriction of the supercoiled closed-circular form.[9] Presumably the nanorod polyplex formation observed here can be explained by the same mechanism as polyplex formation with linear PEG-PLL. The further evaluations are needed to clarify the DNA folding in the nanorod polyplexes. Importantly, the maPEG-PLL bearing the largest maPEG results in the formation of more elongated nanofiber polyplexes. This indicates that the intrapolyplex PEG crowding effect increases with an increase in the exclusion volume of maPEG. As a result, the folding of a DNA molecule is not induced and the polyplex can have nanofiber-like morphology. Also, the topology of pDNA molecules is important for the formation of nanofiber polyplexes. When a supercoiled structure of plasmid DNA is forced to be linear by a restriction enzyme, the polyplexes form spherical aggregates, even with 5k16−71 (Supporting Information, Figure S2).

Finally, the cell-free gene expression, which reflects the efficiency of the transcription and translation process of polyplexes, was evaluated as an effect of the size of the maPEG head on its function. The luciferase activity (luminescence intensity) of the polyplexes was thus measured. Figure 4 shows the relative gene expression of the polyplexes with various maPEG head R_g values of maPEG-PLL. The luciferase activity sharply increased from an R_g of 2 nm. This seems to be related to the elongation of polyplex morphology. PLL without maPEG, that is, the PLL homopolymer formed polyplexes with spherical aggregates. These exhibit low luciferase activity. On the other hand, luciferase activity drastically increased with an increase in the R_g of the maPEG head. Importantly, an increase in R_g of the maPEG head provides an elongation of polyplex morphology from spherical aggregates to nanorods and nanofibers, as shown in Figure 3 and Table 2. These results indicate that the elongated morphology of the polyplexes is advantageous in the tran-

dx.doi.org/10.1021/mz500072k | ACS Macro Lett. 2014, 3, 333−336

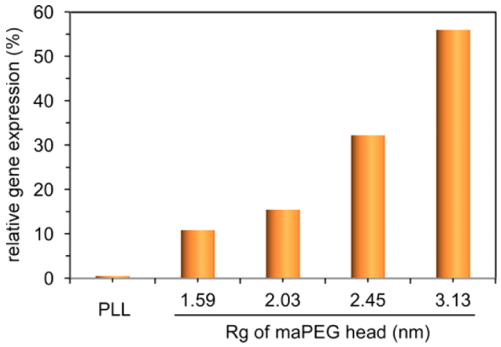

Figure 4. Relative gene expression of the polyplex prepared using maPEG-PLL with various maPEG head R_g values. The relative gene expression is the luciferase activity of the polyplex against that of naked pDNA. The polyplexes were prepared at N/P = 3. The data are presented as the average of three experiments.

scription and translation process of gene expression and the size of the maPEG head in maPEG-PLL influences gene expression by the control of polyplex morphology.

In conclusion, the effect of maPEG size in maPEG-PLL was evaluated in terms of polyplex formation, polyplex morphology and cell-free gene expression. The cooperativity of polyplex formation decreased with the introduction of a maPEG head to a PLL tail. The steric repulsion among the maPEG heads within a polyplex because of the crowding of maPEG heads can induce an elongation of polyplex morphology. Eventually, for the largest maPEG head, the folding of pDNA molecules with charge neutralization was effectively inhibited and the polyplexes had nanofiber morphology. These results indicate that the packaging of the DNA molecule in the polyplex can be controlled by the properties of the maPEG head although the maPEG head does not interact with the pDNA molecule directly. Furthermore, the size of the maPEG part influences the polyplex morphology and also the gene expression. An increase in the size of maPEG provides the most effective inhibition of a decrease in cell-free gene expression. The increase in gene expression is probably induced by the elongation of polyplex morphology. This is first report on the formation of nanofiber polyplex based on the effect of indirectly interacting part with pDNA, although various PEGylated polycations have been studied on their polyplex formation. The use of PAMAM dendron for the branching of multiarm PEG might play an important role in this finding for the effect of the noninteracting block on polyplex morphology. It is expected that the results obtained here can provide valuable knowledge for the design of a nonviral gene vector using synthetic polymers, especially for DNA packaging.

■ ASSOCIATED CONTENT

Ⓢ Supporting Information

Experimental procedures including polymer synthesis, gel retardation assays, AFM observations, and cell-free gene expression assays, GPC charts for maPEGs, and the effect of DNA topology. This material is available free of charge via the Internet at http://pubs.acs.org.

■ AUTHOR INFORMATION

Corresponding Author

*E-mail: harada@chem.osakafu-u.ac.jp.

Notes

The authors declare no competing financial interest.

■ ACKNOWLEDGMENTS

This research was supported by the Ministry of Education, Science, Sports and Culture, Grant-in-Aid for Scientific Research (B) (No. 23300179).

■ REFERENCES

(1) (a) Darling, S. B. *Prog. Polym. Sci.* **2007**, *32*, 1152−1204. (b) Kim, J. K.; Yang, S. Y.; Lee, Y.; Kim, Y. *Prog. Polym. Sci.* **2010**, *35*, 1325−1349. (c) Herr, D. J. C. *J. Mater. Res.* **2011**, *26*, 122−139. (d) Sun, J. T.; Hong, C. Y.; Pan, C. Y. *Soft Matter* **2012**, *8*, 7753−7767. (e) Wu, D.; Xu, F.; Sun, B.; Fu, R.; He, H.; Matyjaszewski, K. *Chem. Rev.* **2012**, *112*, 3959−4015.

(2) (a) Miyata, K.; Christie, R. J.; Kataoka, K. *React. Funct. Polym.* **2011**, *71*, 227−234. (b) Xiong, X. B.; Falamarzian, A.; Garg, S. M.; Lavasanifar, A. *J. Controlled Release* **2011**, *155*, 248−261. (c) Siegwart, D. J.; Oh, J. K.; Matyjaszewski, K. *Prog. Polym. Sci.* **2012**, *37*, 18−37. (d) Duncan, R.; Vicent, M. J. *Adv. Drug Delivery Rev.* **2013**, *65*, 60−70.

(3) Tockary, T. A.; Osada, K.; Chen, Q.; Machitani, K.; Dirisala, A.; Uchida, S.; Nomoto, T.; Toh, K.; Matsumoto, Y.; Itaka, K.; Nitta, K.; Nagayama, K.; Kataoka, K. *Macromolecules* **2013**, *46*, 6585−6592.

(4) (a) Itaka, K.; Kataoka, K. *Curr. Gene Ther.* **2011**, *11*, 457−465. (b) Miyata, K.; Nishiyama, N.; Kataoka, K. *Chem. Soc. Rev.* **2012**, *41*, 2562−2574.

(5) Mao, S.; Neu, M.; Germershaus, O.; Merkel, O.; Sitterberg, J.; Bakowsky, U.; Kissel, T. *Bioconjugate Chem.* **2006**, *17*, 1209−1218.

(6) (a) Harada, A.; Kawamura, M.; Matsuo, T.; Takahashi, T.; Kono, K. *Bioconjugate Chem.* **2006**, *17*, 3−5. (b) Harada, A.; Kawamura, M.; Matsuo, T.; Kimura, Y.; Takahashi, T.; Kojima, C.; Kono, K. *Macromol. Biosci.* **2009**, *9*, 605−612. (c) Harada, A.; Kimura, Y.; Kojima, C.; Kono, K. *Biomacromolecules* **2010**, *11*, 1036−10422. (d) Harada, A.; Kimura, Y.; Kono, K. *ChemBioChem* **2010**, *11*, 1985−1988.

(7) (a) Zdyrko, B.; Varshney, S. K.; Luzinov, I. *Langmuir* **2004**, *20*, 6727−6735. (b) Ostaci, R. V.; Damiron, D.; Al Akhrass, S.; Grohens, Y.; Drockenmuller, E. *Polym. Chem.* **2011**, *2*, 348−354.

(8) Maruyama, A.; Watanabe, H.; Ferdous, A.; Katoh, M.; Ishihara, T.; Akaike, T. *Bioconjugate Chem.* **1998**, *9*, 292−299.

(9) Osada, K.; Oshima, H.; Kobayashi, D.; Doi, M.; Enoki, M.; Yamasaki, Y.; Kataoka, K. *J. Am. Chem. Soc.* **2010**, *132*, 12343−12348.